ResearchGate

See discussions, stats, and author profiles for this publication at: https://www.researchgate.net/publication/234081151

Monte Carlo simulation of homopolymer chains. I. Second virial coefficient

ARTICLE *in* THE JOURNAL OF CHEMICAL PHYSICS · MARCH 2003

Impact Factor: 2.95 · DOI: 10.1063/1.1543940

CITATIONS
13

READS
25

4 AUTHORS, INCLUDING:

Andrey V Dobrynin
University of Akron
124 PUBLICATIONS **4,892** CITATIONS
SEE PROFILE

Michael Rubinstein
University of North Carolina at Chapel Hill
103 PUBLICATIONS **4,879** CITATIONS
SEE PROFILE

Available from: Andrey V Dobrynin
Retrieved on: 23 January 2016

Monte Carlo simulation of homopolymer chains. I. Second virial coefficient

Ian M. Withers
Department of Chemistry, University of North Carolina, Chapel Hill, North Carolina 27599-3290

Andrey V. Dobrynin
Institute of Materials Science and Department of Physics, University of Connecticut, Storrs, Connecticut 06269-3136

Max L. Berkowitz and Michael Rubinstein
Department of Chemistry, University of North Carolina, Chapel Hill, North Carolina 27599-3290

(Received 7 August 2002; accepted 13 December 2002)

The second virial coefficient, A_2, is evaluated between pairs of short chain molecules by direct simulations using a parallel tempering Monte Carlo method where the centers of mass of the two molecules are coupled by a harmonic spring. Three off-lattice polymer models are considered, one with rigid bonds and two with flexible bonds, represented by the finitely extensible nonlinear elastic potential with different stiffness. All the models considered account for excluded volume interactions via the Lennard-Jones potential. In order to obtain the second virial coefficient we calculate the effective intermolecular interaction between the two polymer chains. As expected this intermolecular interaction is found to be strongly dependent upon chain length and temperature. For all three models the θ temperature (θ_n), defined as the temperature at which the second virial coefficient vanishes for chains of finite length, varies as $\theta_n - \theta_\infty \propto n^{-1/2}$, where n is the number of bonds in the polymer chains and θ_∞ is the θ point for an infinitely long chain. Introducing flexibility into the model has two effects upon θ_n; the θ temperature is reduced with increasing flexibility, and the n dependence of θ_n is suppressed. For a particular choice of spring constant an n-independent θ temperature is found. We also compare our results with those obtained from experimental studies of polystyrene in decalin and cyclohexane, and for poly(methyl methacrylate) in a water and *tert*-butyl alcohol mixture, and show that all the data can be collapsed onto a single universal curve without any adjustable parameters. We are thus able to relate both A_2 and the excluded volume parameter v, to the chain interaction parameter z, in a way relating not only the data for different molecular weights and temperatures, but also for different polymers in different solvents. © *2003 American Institute of Physics.* [DOI: 10.1063/1.1543940]

I. INTRODUCTION

The behavior of homopolymer chains at very low concentrations has attracted considerable attention.[1–4] In particular, Monte Carlo (MC) simulations have been used to generate self-avoiding random walks for various model homopolymer systems at infinite dilution.[5–14] In all of these models the monomer–monomer interactions are taken to be of van der Waals type; consisting of a hard-core repulsion and a short-ranged attraction. At high temperatures, or good solvent conditions, repulsive interactions dominate and the polymer swells relative to a random coil. Alternatively at low temperatures, or poor solvent conditions, attractive interactions dominate and chains collapse into dense globules. Observation of isolated macromolecules in the collapsed state in experimental studies is very difficult since in poor solvent conditions the polymer is no longer soluble and precipitates from solution. Phase separation can, in some cases, be avoided by considering systems which are sufficiently dilute.[15] At intermediate temperatures, between the good and poor solvent regimes, the polymer is in a θ-solvent condition, i.e., at temperatures close to the θ point.

The true θ point (θ_∞) is defined as the temperature at which the second virial coefficient between two infinitely long chains is zero.[1] This definition is, of course, not practical since neither experiments nor computer simulations can be performed upon infinitely long chains, and the most common empirical definition of the θ point is the temperature at which the second virial coefficient between chains of finite length is zero[4] (we use the notation θ_n to represent the θ temperature of a chain of finite length). A temperature is thus obtained which may depend upon the number of bonds in the chain, n, and the true θ temperature is obtained in the limit

$$\theta_\infty = \lim_{n\to\infty} \theta_n . \tag{1}$$

Previously, several computer simulation studies have evaluated the θ point following this definition of the θ temperature.[6–8,10,12,14] These models display behavior different from that observed in experiment; namely a strong n dependence of θ_n, whereas experimental studies find either a very weak n dependence[16] or no n dependence.[17] Renormalization group calculations[4] show that n dependence of θ_n is to be expected, with a stronger n dependence being predicted with increasing three-body interaction parameter. The models typically used[6–8,10,12] in computer simulation studies have a much smaller aspect ratio of their Kuhn segments than real polymers do, resulting in the three-body repulsions being an

 © 2003 American Institute of Physics

order of magnitude stronger in the model systems.[18] The experimentally observed n independence of θ_n could, therefore, be due to relatively weak three-body interactions being present in real polymeric materials.

It is, therefore, a worthy task to attempt to find a model polymer chain which exhibits an n independent or weakly n-dependent θ temperature, such that the results of computer simulations will be closer to experimental ones. We note that determination of the θ temperature from conformational properties of lattice models of polymer chains indicates that the n dependence of θ_n may be suppressed by considering a model with flexible bonds.[19] Introducing a variable bond length into the model is computationally simpler than increasing the aspect ratio of the Kuhn segments; allowing the bond length to vary requires only one bonded energy term while increasing the chain stiffness requires two or three bonded terms (the bond length, the valence angle and possibly the torsion angle). In this paper we, therefore, evaluate the second virial coefficient, A_2, for three types of model polymer chains, one with rigid bonds and two with flexible bonds of different stiffnesses, containing $(n+1)=2$, 4, 8, and 16 monomers, using a new method inspired by the theoretical work of Grosberg and Kuznetsov.[20] It will be shown that an appropriate choice of parametrization of the flexible bond may lead to an n-independent θ temperature. The results obtained from a study of the chain dimensions of this model polymer, along with comparison with theoretical predictions, are presented in Paper II.[18]

The remainder of this paper is organized as follows: In the next section we describe our new method for evaluating the second virial coefficient. In Sec. III we consider the application of the method to the simple case of a pair of Lennard-Jones particles where results obtained by simulation are compared with the *exact* numerical evaluation. Results obtained for short homopolymer chains, along with comparison with previous simulation studies of similar models, are presented in Sec. IV. We also compare our numerical results of the second virial coefficient with experimental results in Sec. IV, and show that the simulation data may be collapsed onto a universal curve with the experimental data without the use of any adjustable parameters. Finally our conclusions and discussion are given in Sec. V.

II. DESCRIPTION OF THE METHOD

The second virial coefficient, A_2, of a polymer solution is an important property, since it describes the interactions between pairs of molecules, and has been the subject of numerous theoretical and experimental studies.[3,4] An expression for the second virial coefficient in terms of the interaction potentials can be obtained from standard statistical mechanics as[21]

$$A_2 = -\frac{2\pi N_A}{M^2}\int_0^\infty R^2\left[\exp\left(-\frac{U(R)}{k_BT}\right)-1\right]dR, \tag{2}$$

where M is the molar mass of the molecules and $U(R)$ is considered as an effective intermolecular interaction between the chain molecules whose centers of mass are separated by a distance R, i.e., a potential of mean force which is solvent and temperature dependent and corresponds to an average over all possible chain conformations (i.e., the average over all internal conformations of each chain *and* over all orientations of each chain relative to the intermolecular vector between the centers of mass of the two molecules, **R**). The task of evaluating the second virial coefficient between two chain molecules by computer simulation thus reduces to evaluating $U(R)$.

The most popular methods of evaluating $U(R)$ is based upon the idea that the effective intermolecular interaction may be expressed as the average of the intermolecular interaction energy, $U_{12}(R,\alpha_1,\alpha_2)$, between chain 1 in conformation α_1 and chain 2 in conformation α_2,[3]

$$U(R) = -k_BT\ln\left\langle \exp\left(-\frac{U_{12}(R,\alpha_1,\alpha_2)}{k_BT}\right)\right\rangle_{\alpha_1,\alpha_2}, \tag{3}$$

where $\langle\ \rangle_{\alpha_1,\alpha_2}$ denotes an average over conformations of two chains without interchain interactions. The average in Eq. (3) is typically evaluated[6,7] by generating many pairs of chains of the desired length independently and calculating $U_{12}(R,\alpha_1,\alpha_2)$ between the two chains at many random separations and orientations relative to each other. This method has become popular since it has been shown to be an efficient method for evaluating $U(R)$ in good solvent conditions. In poor solvent conditions, where the two chains collapse into a single dense globule, this method is not very efficient due to the very low probability of generating two chains independently which will entwine with each other. Furthermore this method is inefficient for systems containing solvent, since the solvent particles would have to be equilibrated around the two chains after they are generated but before calculating the intermolecular interaction energy. This strategy would be very time consuming and render this method highly inefficient for examining the effects of solvent properties (for example, density) upon the second virial coefficient. It is therefore desirable to have a method for evaluating $U(R)$ during the course of a direct simulation of two polymer chains.

To overcome the sampling problem we performed direct simulations of the two interacting polymers which center of masses are coupled via a spring such that the probability of finding the two chains at a distance R apart becomes

$$P_s(R) = C\exp(-(U(R)+U_s(R))/k_BT), \tag{4}$$

where C is the normalization constant and $U_s(R) = kR^2/2k_BT$ is the contribution to the potential energy from the spring with spring constant k. The introduction of the additional interaction potential between chains allows us to sample the configurational spaces of the two chains in Metropolis sense—generating the most probable configurations of two interacting chains.[22] Since the energy associated with the spring increases rapidly with increasing R, it is possible to choose a value of the spring constant, k, such that the probability of finding the two chains beyond the range of the intermolecular interaction decreases rapidly with increasing R, thus placing a restriction upon how far apart the two chains may move from each other. This restriction allows the probability $P_s(R)$ to be accumulated by computer simula-

tions whose run times are not prohibitively excessive, since we are now only interested in accumulating data up to distances where the probability of finding the two chains becomes negligibly small. It should be noted that the choice of the spring constant, k, is very important since too stiff a spring will perturb the chain conformations, altering the resulting form of the intermolecular interaction $U(R)$. Alternatively, too weak a spring will allow the polymers to move further apart than is necessary, leading to longer simulation runs to obtain the probability histograms with a desired degree of accuracy.

III. LENNARD-JONES PARTICLES

To demonstrate the validity of this method to calculate the effective intermolecular interaction, $U(R)$, and the second virial coefficient, A_2, we apply the new method to a pair of particles interacting via the truncated-shifted Lennard-Jones potential,

$$U_{\mathrm{LJ}}(r) = \begin{cases} 4\epsilon\left[\left(\frac{\sigma}{r}\right)^{12}-\left(\frac{\sigma}{r}\right)^{6}\right]-4\epsilon\left[\left(\frac{\sigma}{r_c}\right)^{12}-\left(\frac{\sigma}{r_c}\right)^{6}\right], & r<r_c, \\ 0, & r\geqslant r_c, \end{cases} \tag{5}$$

where r is the distance between the two particles, σ is the (effective) diameter of the particle, ϵ is the depth of the attractive minima, and r_c is the cutoff radius ($=2.5\sigma$). Since this is a particularly simple problem [$U(R)$ should equal $U_{\mathrm{LJ}}(r)$] it is our aim in this section to demonstrate the applicability of this method for evaluation of $U(R)$ by computer simulation, while comparing our results with analytical functions and the *exact* numerical integration of Eq. (2).

To accumulate the probability $P_s(R)$ we use the Metropolis Monte Carlo method.[22] Trial conformations were generated by randomly choosing one of the two particles and then displacing it in the x, y, and z directions by random distances. The maximum displacement was kept fixed at 0.1σ throughout the simulations. The spring constant, k, linking the two particles was chosen such that the average distance between particles without the Lennard-Jones interaction was 5σ. The probability $P_s(R)$ was collected by accumulating the distance between the two particles into a histogram whose bins were of width $\delta R=0.02\sigma$. In order to improve the sampling process we have also employed the parallel tempering method.[23] Our simulations were performed on nine processors with the temperature of each simulation being linearly distributed over the range $k_BT/\epsilon=1.0$ to 5.0. Temperature exchanges between systems were attempted every 2×10^3 attempted particle moves. In total 2×10^7 trial moves were attempted at each temperature.

In Fig. 1 we illustrate the procedure by which the probability, $P_s(R)$, obtained from a simulation at temperature $k_BT/\epsilon=3.0$ was converted into the effective intermolecular interaction. In Fig. 1(a) the points show $P_s(R)$ obtained from the simulation and the solid line represents the analytically expected probability distribution [Eq. (4)]. The agreement between the simulation data and the analytical function is excellent, indicating that a sufficient number of trial conformations have been generated. In order to obtain the relative probability of finding two particles at a distance R apart due solely to the effective intermolecular interaction,

$$P(R)=\exp\left(-\frac{U(R)}{k_BT}\right), \tag{6}$$

it is necessary to remove the contribution due to the spring.

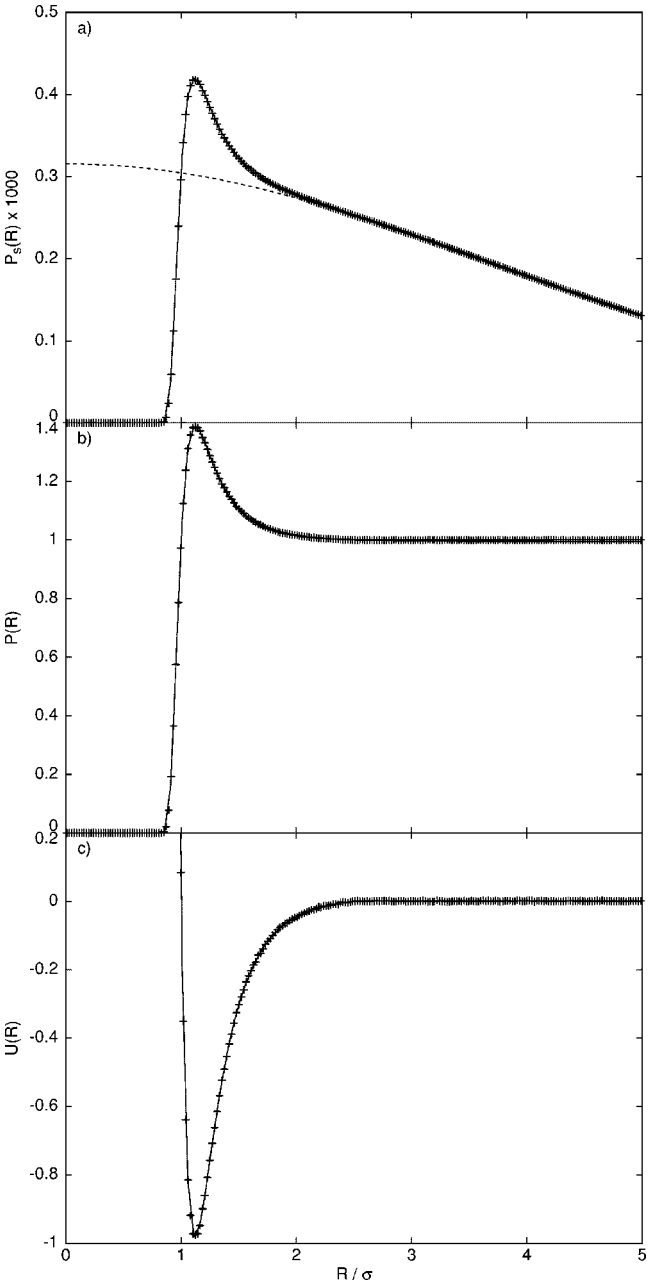

FIG. 1. Manipulation of the simulated probability distribution $P_s(R)$ to obtain the intermolecular interaction $U(R)$ for a pair of Lennard-Jones particles at a temperature of $k_BT/\epsilon=3.0$. Results from the simulation are shown as points (+) and analytic functions are shown by solid lines. Panel (a) shows the probability distribution function $P_s(R)$ obtained from the simulation, the dashed line shows the contribution from the spring coupling the centers of masses together, panel (b) shows the probability distribution function $P(R)$ after removal of the contribution from the spring, and panel (c) shows the resulting intermolecular potential, $U(R)$. Error bars are smaller than the point size.

TABLE I. Values of the second virial coefficient (A_2) in units of σ^3 for a pair of Lennard-Jones particles evaluated at various temperatures by numerical integration of Eq. (2) where $U(R)$ is evaluated from Eq. (5) and from simulation. Numbers in parentheses in the simulation column represent the statistical error to the last two decimal places.

k_BT/ϵ	A_2M^2/N_A (analytical)	A_2M^2/N_A (simulation)
1.0	−4.167	−4.183(75)
1.5	−1.778	−1.779(62)
2.0	−0.771	−0.748(61)
2.5	−0.224	−0.204(41)
3.0	0.115	0.113(41)
3.5	0.343	0.323(61)
4.0	0.506	0.510(26)
4.5	0.627	0.628(17)
5.0	0.720	0.730(30)

To accomplish this it is noted that beyond the range of the intermolecular interaction the only contribution to $P_s(R)$ comes from the spring term, i.e., $P_s(R) = C\exp(-U_s(R)/k_BT)$ for $R > r_c$, where C is a constant of proportionality arising due to the difference between the normalization of the total probability and the probability due only to the spring. The numerical value of C may be obtained by a least-squares-fitting procedure[24] to $P_s(R)$ over the range $R > r_c$ [as shown by the dashed line in Fig. 1(a)]. Division of $P_s(R)$ by $C\exp(-U_s(R)/k_BT)$ gives the relative probability of finding the two particles at distance R apart due to the effective intermolecular interaction, $P(R)$ [Fig. 1(b)], which is normalized correctly to allow the effective intermolecular interaction to be obtained, i.e., $P(R)=1$ for large R. Finally, the effective intermolecular interaction is given by the relation $U(R) = -k_BT\ln(P(R))$. Figure 1(c) clearly shows that this process has lead us back to the Lennard-Jones potential given by Eq. (5) [the points show the simulation data and the solid line shows Eq. (5)].

In Table I we present the values of the second virial coefficient obtained by numerical integration of Eq. (2),[24] where $U(R)$ is given analytically [Eq. (5)] and has been determined from simulation. The step size between points used for the *exact* numerical integration was taken to be two orders of magnitude smaller than that used in the simulation. The error estimates quoted for the simulation results were obtained by performing the numerical integration using an intermolecular interaction obtained from the probability distributions function $P_S(R) \pm s(R)$ [where $s(R)$ is the statistical error obtained by the block averaging technique].[22] The results quoted in Table I clearly demonstrate the equivalence, within the statistical error, of the values of the second virial coefficient obtained from the simulation and by the *exact* numerical integration, illustrating that this method provides an accurate route to calculate the second virial coefficient.

IV. SHORT POLYMER CHAINS

A. Model

Having demonstrated the applicability of the new method for determining the effective intermolecular interaction and the second virial coefficient for the simple case of two Lennard-Jones particles, we now present the results for two short polymer chains. We consider three models of polymer chains. All the models account for the excluded volume interaction by the truncated-shifted Lennard-Jones potential [Eq. (5)]. The difference between these models is how connectivity of the chain is assured. In the first case all bond lengths are kept fixed at σ. This type of model has been considered previously by Harismiadis and Szleifer,[7] although it should be noted that their model differs from ours slightly; we employ the truncated-shifted Lennard-Jones potential, while Harismiadis and Szleifer employed only the truncated Lennard-Jones potential, i.e., an energy discontinuity was present in Ref. 7 at $r = r_c$. The other two models have flexible bonds. The interaction energy between adjacent monomers is given by the sum of the truncated-shifted Lennard-Jones potential [Eq. (5)] and the finitely extensible nonlinear elastic (FENE) potential,

$$U_{\mathrm{FENE}}(r) = -\frac{1}{2}k_{\mathrm{FENE}}R_0^2\ln\left[1-\frac{r^2}{R_0^2}\right], \tag{7}$$

where k_{FENE} is an adjustable spring constant and R_0 is the maximum extension of the bond, at which the interaction energy becomes infinite. In the present study we used $R_0 = 2\sigma$ and $k_{\mathrm{FENE}} = 10.0\epsilon/\sigma^2$ and $30.0\epsilon/\sigma^2$.

Different methods are used to generate trial conformations for each of these models. For the model with rigid bonds a trial move is generated by selecting a monomer at random and then rotating it by a random amount about the axis formed by the line that joins the centers of mass of the two adjacent sites (or the next two innermost sites if a monomer at the end of the chain was selected). The extent of the rotation was chosen uniformly in the interval 0 to 2π. For the model with flexible bonds trial conformations are generated by selecting a monomer at random and then displacing it by random amounts in the x, y, and z directions, generated uniformly between -0.1σ and 0.1σ. As with the two Lennard-Jones particles considered in the preceding section, the trial move for both models is accepted or rejected according to the Metropolis acceptance criterion.[22]

To choose the value of the spring constant, k, connecting the centers of mass of the two polymers we conducted a preliminary series of simulations, for all three models using the longest chain length, with chains containing $n=15$ bonds, at the highest dimensionless temperature, $k_BT/\epsilon = 5.0$, considered in this work, since the unfavorable effects associated with the use of too strong a spring are likely to be more noticeable in good solvent conditions as the chains are larger (swollen) and are expected to repel each other. The simulations were started with a small spring constant, corresponding to an average extension of the spring without intermolecular interactions of 10σ. The spring constant was then increased, such that the average extension of the spring was reduced by integer values of σ, until deviations were observed in the average end-to-end distance and radius of gyration. For all three models considered, such deviations became apparent for a spring constant corresponding to an average extension of the spring of 3σ. The remainder of the simulations were therefore performed using a spring constant giving an average spring extension of 4σ. It is also noted that

the root-mean-square radius of gyration for the $n=15$ chains at this temperature is approximately 2.25σ.

The simulations were started by generating two random self-avoiding chain conformations independently, where the initial bond length was taken as σ for all the models. The two chains were placed such that their centers of mass were 5σ apart. The system was then checked for intermolecular overlap (an overlap is defined as two monomers being separated by a distance smaller than σ) and if monomers were found to overlap then two new conformations were generated and the process was repeated until a nonoverlapping conformation was generated. The system was then equilibrated for 10^5 MC sweeps, where one MC sweep consists of one attempted move per monomer, i.e., $2\times(n+1)$ moves. The probability distribution, $P_s(R)$, was accumulated over an additional 10^7 MC sweeps. Parallel tempering was once again employed to improve the efficiency of the sampling process. The majority of the simulations were performed using nine processors with the temperature of each simulation being linearly distributed over the range $k_BT/\epsilon=1.0$ to 5.0. An additional three processors (12 in total) were used for the chains with $k_{\mathrm{FENE}}=10.0\epsilon/\sigma^2$, with these extra simulations being assigned temperatures very close to the θ temperature to confirm the observation of preliminary simulations using only nine processors. Temperature exchanges were attempted every 10^3 MC sweeps. Removal of the spring contribution to $P_s(R)$ was once again achieved by fitting $P_s(R)$ to $C\exp(-U_s(R)/k_BT)$ for distances beyond the range of the intermolecular interaction. Since the range of the intermolecular potential is not known *a priori*, we perform fits in the range $R>r_l$, where r_l is the lowest integer multiple of σ which yields the same value of the coefficient C, within error estimates, when compared with the values obtained from fits performed with larger lower bounds. Via this procedure, we find $r_l=3\sigma$, 4σ, 5σ, and 7σ for $n=1$, 3, 7, and 15, respectively.

B. Intermolecular potential

In Fig. 2 we show the effective intermolecular interaction between polymer chains as a function of distance between their centers of mass for chains with rigid bonds of length $n=15$ at five different temperatures. It can be clearly seen that the strength, and form, of the effective intermolecular interaction shows a strong variation with temperature. At the highest temperature considered, $k_BT/\epsilon=5.0$, $U(R)$ is positive for all R, i.e., the intermolecular interaction is purely repulsive, indicative of good solvent conditions, where the chains swell and repel each other. As has been reported previously,[6,7] the interaction energy at zero separation between the centers of mass of the two chains is positive and finite. This behavior occurs since, unlike the monomeric case, it is possible for the centers of mass of polymers to overlap without resulting in an overlap of any monomers. At the lowest temperature considered, $k_BT/\epsilon=1.0$, $U(R)$ is negative for all R, i.e., the intermolecular interaction is purely attractive, indicative of poor solvent conditions where the monomers attract each other and the chains collapse into a globular state. In this case, it is interesting to note that for separations smaller than $\sim 1.5\sigma$ the intermolecular interaction is approximately constant, with no upturn being observed with decreasing R. This behavior tends to indicate that the two polymer chains attract each other so strongly that they coalesce in a single globule. This type of behavior has been inferred previously,[6] however, the statistical error observed in this previous study (see Fig. 5 of Ref. 6) is considerably worse than ours, due to the very low probability of growing two chains independently that will entwine with each other in a single dense globule, illustrating a clear advantage of employing our method to study behavior in poor solvent conditions. That said, the current method yields a larger statistical error for small separations in good solvent conditions, since the interchain repulsion makes these small separations difficult to sample. For temperatures between these two limiting cases, $U(R)$ displays behavior similar to that observed previously;[7] an increase in the intermolecular interaction between molecules with overlapping centers of mass with increasing temperature, arising since the repulsion between the chains increases as the chains swell, and the observation of an attractive minimum, which becomes less deep and occurs at larger separations with increasing temperature, once again due to the increased repulsion associated with increasing temperature. Similar behavior is also observed for the models with flexible bonds.

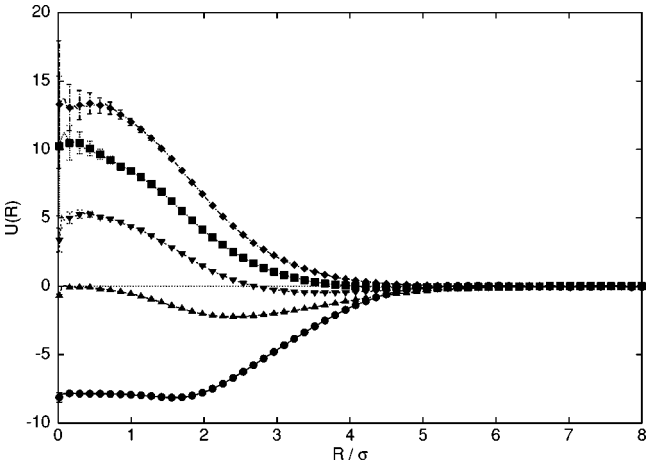

FIG. 2. Effective intermolecular interaction ($U(R)$) vs distance between the center of mass of the two chains (R) for $n=15$ with rigid bonds at temperatures of $k_BT/\epsilon=1.0$ (●), 2.0 (▲), 3.0 (▼), 4.0 (■), and 5.0 (♦). For clarity only every sixth data point is shown, although the lines pass through all the data points.

Figure 3 shows the effective intermolecular interaction between two chains at temperatures of $k_BT/\epsilon=2.0$ and 4.0 for the model with rigid bonds and different chain lengths. As will be confirmed shortly, these temperatures correspond to poor and good solvent conditions, respectively, for all the chain lengths considered. For both solvent conditions, increasing the chain length reduces the repulsion at zero separation from infinity for the monomeric case to approximately 11ϵ and 0 for good and poor solvent conditions, respectively, for the longest chain considered here, $n=15$. This behavior has been observed previously in computer simulation studies,[6,7] but is, however, unexpected following the mean field theory of Flory and Krigbaum.[25] In this mean field

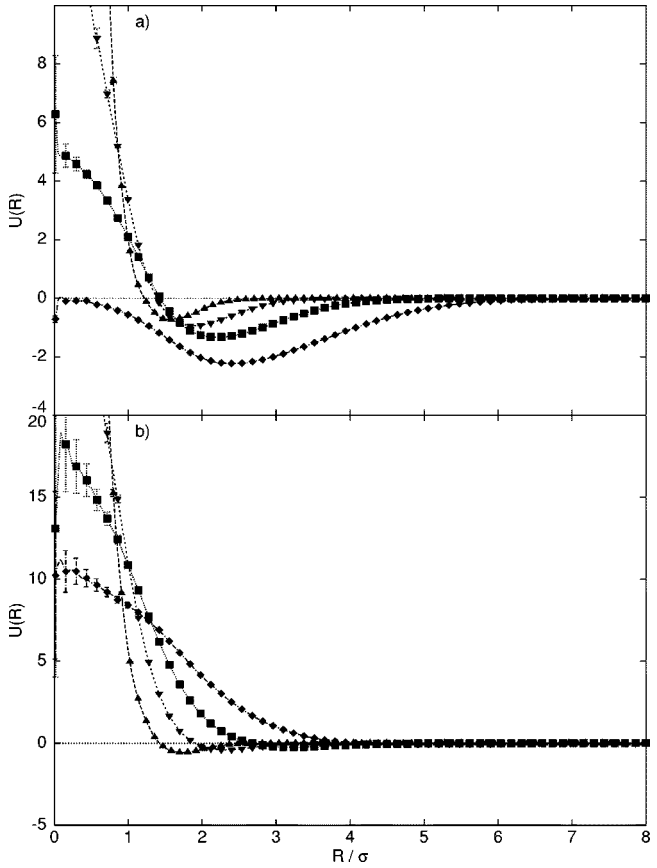

FIG. 3. Effective intermolecular interaction ($U(R)$) vs distance between the center of mass of the two chains (R) for $n=1$ (▲), 3 (▼), 7 (■) and 15 (♦) at temperatures of (a) $k_BT/\epsilon=2.0$ and (b) 4.0 for the model with rigid bonds. For clarity only every sixth data point is shown, although the lines pass through all the data points.

theory the free energy of interaction is proportional to the average number of contacts between monomers within the overlap region. The average number of contacts was taken to be the product of the number of monomers of one chain in the overlap region ($\propto n$) and the contact probability for each of these monomers ($\propto$ monomer concentration within the coils $\propto nR^{-3}\propto n^{-4/5}$), which results in the free energy of interaction between two chains in good solvent conditions at short distances increasing as $k_BTn^{1/5}$. The Flory–Krigbaum theory, however, assumes that the monomers are uniformly distributed within the volume of a polymer coil. This assumption is not valid since chain connectivity ensures that each monomer is surrounded by a *cloud* of monomers which are close along the chain. As a result, when two monomers from different chains are in contact their neighboring monomers along the chain backbone are also likely to be in contact, which leads to an increased effective repulsion between chain segments and therefore to a reduction of the contact probability. Following this argument Grosberg *et al.*[26] showed that accounting for chain connectivity reduces the contact probability ($\propto n^{-1}$), which results in the free energy of interaction at short distances being simply proportional to k_BT and independent on the number of monomers n. Since we have only considered short chains in Fig. 3, such that the interaction energy at zero separation is decreasing with increasing n, we have calculated the probability of two independently grown athermal chains sharing a common center of mass without any molecular overlaps by generating 10^6 pairs of hard sphere chains whose bond length is equal to the diameter of the monomers. These simulations show that while the probability of generating nonoverlapping configurations with common center of masses increases (i.e., interaction energy decreases) with increasing n, the probability, and therefore the interaction energy, do appear to be saturating at a constant value for large n. These observations are consistent with our, and previous,[6,7] simulation results which display a rapidly decreasing $U(0)$ for short chains, and the predicted n independence of $U(0)$ for large n.

Figure 3 also shows that the location and depth of the attractive minimum vary with chain length and solvent condition. In both good and poor solvent conditions the location of the minimum is shifted to larger separation as the chain length is increased, reflecting the larger size of the polymer chains in both the coil and globule states. The depth of the attractive well depends, however, upon the temperature. In good solvent conditions the depth of the minimum decreases with increasing chain length, indicating that increasing chain length results in stronger repulsive interactions between the coils. Alternatively, in poor solvent conditions the depth of the minimum increases with increasing chain length, indicating that increasing chain length results in stronger attractive interactions between the globules. The minima we observed at nonzero separations R in both good and poor solvent conditions are most likely to be artifacts of the short chain lengths employed in the current study. In good solvent conditions we anticipate that as the chain length is increased the depth of the minimum will decrease further, such that for sufficiently long chains no minimum will be observed. In poor solvent conditions we expect that the interaction energy at short distances will be reduced as the two chains coalesce in a single dense globule and an approximately constant attractive energy should be observed (the strength of which is determined by surface effects and should scale as $n^{2/3}$). Clearly the chains considered here are too short for these predictions to be confirmed, and as a result further simulations are certainly warranted. That said, the trends reported here, within good solvent conditions, are in good agreement with the results of Harismiadis and Szleifer,[7] although we note that our interaction energy, for a chain of length $n=15$ at $k_BT/\epsilon=4.0$, at zero separation is larger, by approximately 1.5ϵ. Although no error estimates are quoted in Ref. 7, this deviation can easily be accounted for, arising due to our use of the truncated-shifted Lennard-Jones potential. Once again, behavior similar to that of the rigid bond model was observed for the models with flexible bonds.

C. Second virial coefficients and θ temperatures

In Fig. 4 we show the second virial coefficient, A_2, obtained by numerical integration of Eq. (2) [where $M=(n+1)m_0$, with m_0 being the molar mass of a monomer], as a function of temperature for chain lengths varying from $n=1$ to 15 for all three models. Error estimates were obtained by performing numerical integration from the effective inter-

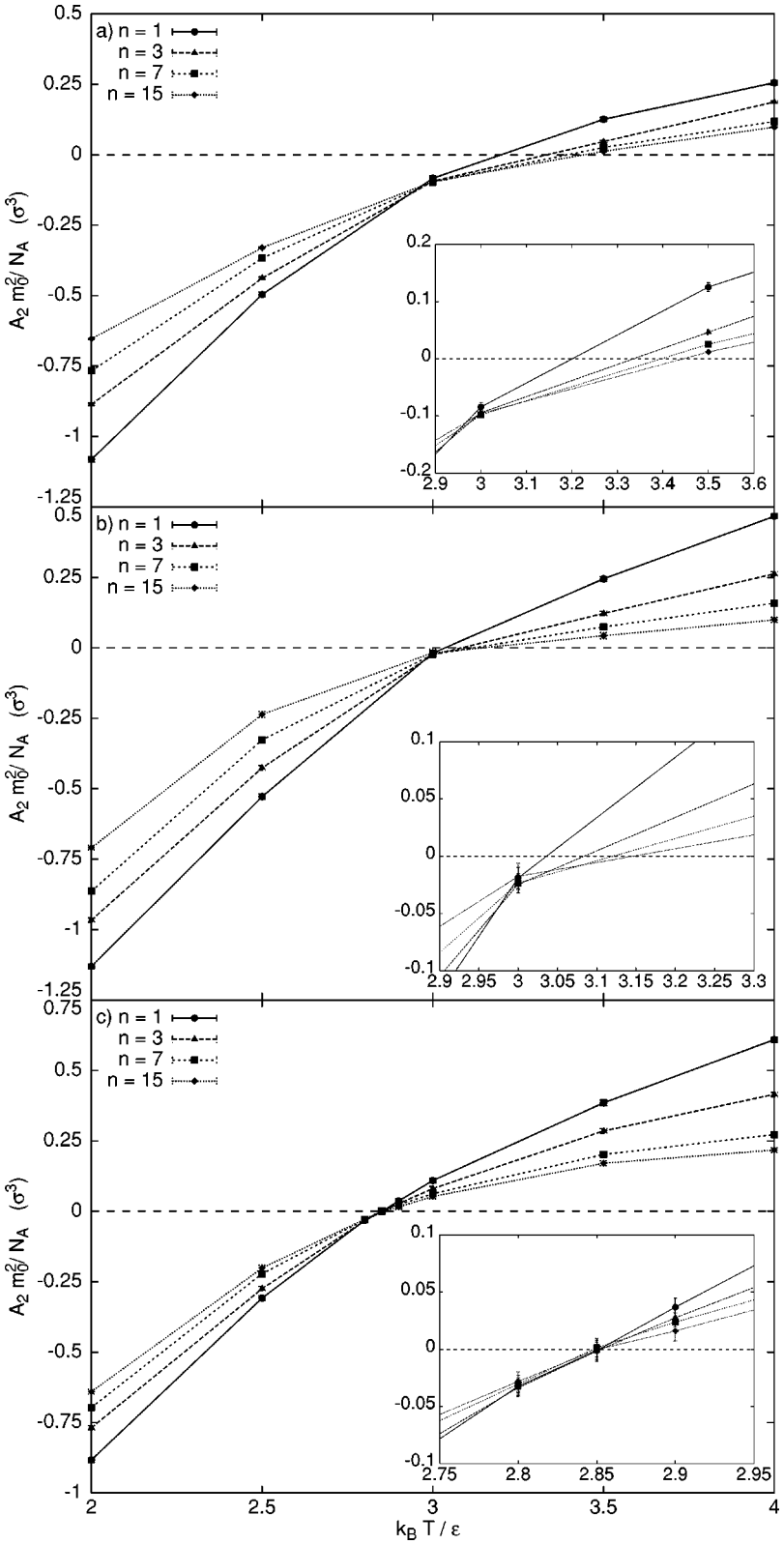

FIG. 4. Second virial coefficient (A_2) as a function of temperature for (a) the model with rigid bonds, (b) the model with flexible bonds and $k_{\mathrm{FENE}} = 30\epsilon/\sigma^2$, and (c) the model with flexible bonds and $k_{\mathrm{FENE}} = 10\epsilon/\sigma^2$ for various chain lengths, $n = 1$ (●), 3 (▲), 7 (■), and 15 (◆).

molecular interactions determined from the probability distributions $P_s(R) \pm s(R)$. The qualitative behavior of the second virial coefficient with temperature is the same for all molecular weights and is similar for all three models. At high temperatures the second virial coefficient is positive, clearly showing that repulsive interactions dominate between the two chains. A_2 decreases with decreasing temperature, indicating that attractive interactions start to play a more important role. All the curves show a point where the second virial coefficient vanishes. This is the θ temperature, θ_n. For the models with rigid bonds and flexible bonds with $k_{\mathrm{FENE}} = 30\epsilon/\sigma^2$, θ_n is dependent upon the chain length, but for the model with flexible bonds and $k_{\mathrm{FENE}} = 10\epsilon/\sigma^2$, θ_n remains constant (within numerical error) independent of chain

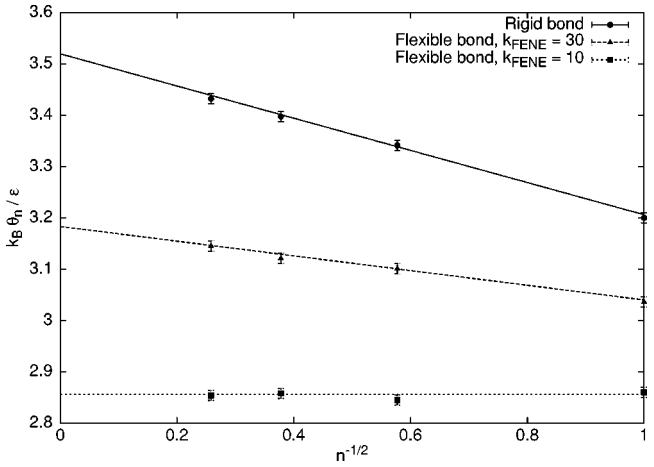

FIG. 5. θ temperature ($k_B\theta_n/\epsilon$) as a function of chain length ($n^{-1/2}$) for the model with rigid bonds (●) and the model with flexible bonds and $k_{\mathrm{FENE}}=30\epsilon/\sigma^2$ (▲) and $k_{\mathrm{FENE}}=10\epsilon/\sigma^2$ (■). The lines show least squares fits to the simulation data.

length. Below the θ temperature, A_2 displays a negative value, indicative of poor solvent conditions where molecular attraction is dominant.

In order to examine the chain length dependence of the θ point we note that previous simulation studies have shown that θ_n varies as $n^{-1/2}$,[8,27,28] although more sophisticated scaling relations have also been used.[10] In Fig. 5 we plot θ_n versus $n^{-1/2}$ for all three models. For the model with rigid bonds, linear dependence is clearly observed, and a least squares fit of the form

$$k_B\theta_n/\epsilon = Bn^{-1/2} + k_B\theta_\infty/\epsilon \tag{8}$$

yields values of $B=-0.31\pm0.03$ and $k_B\theta_\infty/\epsilon=3.52\pm0.01$. Our value of the θ temperature for an infinitely long chain is considerably less than that obtained by Harismiadis and Szleifer[7] (~ 3.9), however, the discrepancy seems likely to be due to our use of the truncated-shifted Lennard-Jones potential, since, as we have already shown, the shifted potential enhances the repulsive contribution to the intermolecular interaction, in turn lowering the temperature at which the second virial coefficient vanishes. That said, we concede that this estimate of θ_∞ has been obtained using data from short chains, and that the value quoted above may be modified by considering longer chains and/or a more sophisticated scaling analysis. Figure 5 also shows the introduction of flexible bonds into the model results in a reduction of both θ_n and θ_∞, such that $k_B\theta_\infty/\epsilon=3.183\pm0.008$ and 2.856 ± 0.006 for $k_{\mathrm{FENE}}\sigma^2/\epsilon=30$ and 10, respectively, along with a suppression of the n dependence of θ_n, $B=-0.14\pm0.01$ and 0.01 ± 0.01 for $k_{\mathrm{FENE}}\sigma^2/\epsilon=30$ and 10, respectively.

To compare our simulation results with experimental results we attempt to collapse our data for the three different model polymers onto a single universal curve with experimental data. To achieve this we note that in the θ regime the interaction energy between two overlapping chains is smaller than the thermal energy, such that the chains interpenetrate each other and the monomers interact directly. The second virial coefficient is therefore proportional to the excluded volume v of a Kuhn segment,[31]

$$A_2=\frac{N_A v}{2M_0^2}, \tag{9}$$

where M_0 is the molar mass of a Kuhn segment and N_A is the Avogadro's number. Let us introduce the chain interaction parameter z_{th} that is the square root of the number of thermal blobs per chain

$$z_{\mathrm{th}}=\left(\frac{N}{N_{\mathrm{th}}}\right)^{1/2}, \tag{10}$$

where

$$N_{\mathrm{th}}=\left(2C_1\frac{b^3}{v}\right)^2 \tag{11}$$

is the number of Kuhn segments in a thermal blob and C_1 is a numerical constant. This interaction parameter z_{th} can therefore be written in terms of the length of a Kuhn segment b and its excluded volume v

$$z_{\mathrm{th}}=\frac{1}{2C_1}\frac{v}{b^3}N^{1/2}. \tag{12}$$

Combining this expression with Eq. (9) one can obtain the relation between second virial coefficient A_2 and the interaction parameter z_{th},

$$A_2=C_1\frac{N_A b^3}{M_0^{3/2}M^{1/2}}z_{\mathrm{th}} \quad \text{for } z_{\mathrm{th}}<1. \tag{13}$$

In good solvents the chains repel each other strongly and do not interpenetrate. Since the volume excluded by a chain is of the order of its pervaded volume, R^3,

$$A_2\propto\frac{N_A R^3}{M^2}, \tag{14}$$

and the relative swelling of the chains in good solvents is

$$\frac{R}{bN^{1/2}}\propto z_{\mathrm{th}}^{0.176} \tag{15}$$

the second virial coefficient in the good solvent regime is given by

$$A_2\propto\frac{N_A b^3}{M_0^{3/2}M^{1/2}}z_{\mathrm{th}}^{0.528} \quad \text{for } z_{\mathrm{th}}>1. \tag{16}$$

Combining Eqs. (13) and (16) and rearranging to obtain dimensionless quantities one can write

$$A_2M^{1/2}\frac{M_0^{3/2}}{N_A b^3}=C_1\begin{cases} z_{\mathrm{th}} & z_{\mathrm{th}}<1 \quad (\theta \text{ solvent}),\\ z_{\mathrm{th}}^{0.528} & z_{\mathrm{th}}>1 \quad (\text{good solvent}).\end{cases} \tag{17}$$

Taking into account the linear dependence of excluded volume parameter v on the effective temperature

$$v=2C_1C_2b^3\left(\frac{T-\theta_n}{T}\right) \tag{18}$$

we can relate the interaction parameter z_{th} to the reduced temperature

$$z_{\mathrm{th}}=C_2N^{1/2}\frac{T-\theta_n}{T}, \tag{19}$$

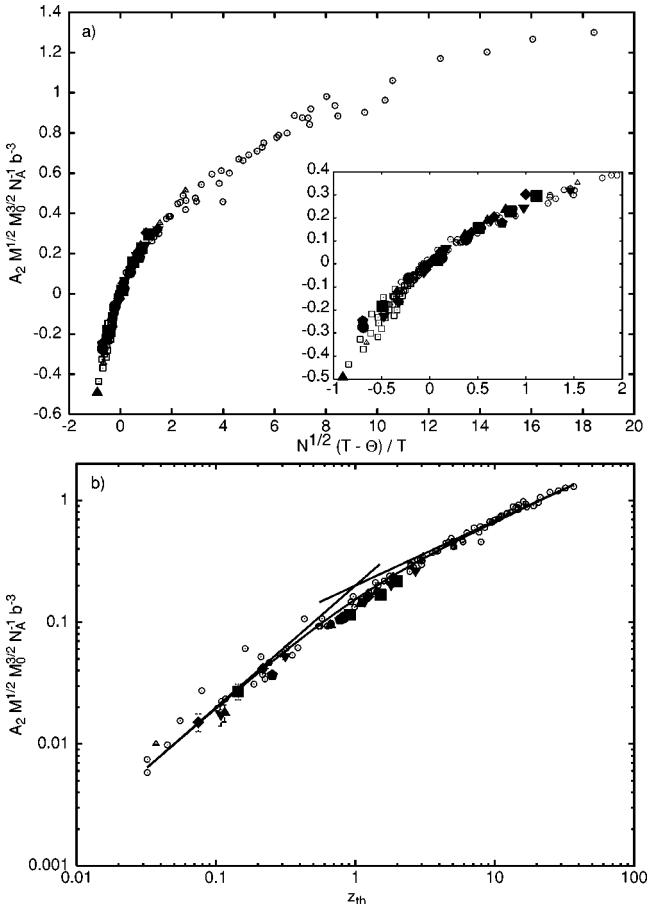

FIG. 6. (a) Universal curve of $A_2M^{1/2}M_0^{3/2}N_A^{-1}b^{-3}$ vs $N^{1/2}(T-\theta_n)/T$ for polystyrene (open symbols) in decalin (Ref. 16) (circles) and cyclohexane (Ref. 29) (squares), poly(methyl methacrylate) in water+*tert*-butyl alcohol (Ref. 30) (triangles) and our simulation data (larger filled symbols); $n=7$ (squares) and 15 (up-triangles) for the model with rigid bonds, $n=7$ (down-triangles), and 15 (diamonds) for the model with flexible bonds and $k_{\mathrm{FENE}}=30\epsilon/\sigma^2$, and $n=7$ (circles) and 15 (pentagons) for the model with flexible bonds and $k_{\mathrm{FENE}}=10\epsilon/\sigma^2$. Inset shows expanded scale of the range covered by the simulation data. (b) Universal curve of $vN^{1/2}b^{-3}$ vs z_{th}. Symbol have the same meaning as in panel (a). The solid lines show the best fits $vN^{1/2}b^{-3}=0.26z_{\mathrm{th}}$, $vN^{1/2}b^{-3}=0.26z_{\mathrm{th}}^{0.528}$, and the crossover function [Eq. (23)].

where C_2 is another numerical constant. Therefore one expects the universal relation between second virial coefficient A_2 and reduced temperature.

In Fig. 6(a) we plot $A_2M^{1/2}M_0^{3/2}N_A^{-1}b^{-3}$ versus $N^{1/2}(T-\theta_n)/T$ for experimental results obtained from polystyrene in decalin[16] and cyclohexane,[29] poly(methyl methacrylate) in a water and *tert*-butyl alcohol mixture,[30] and our simulation data. The values of M_0, b, and θ_n used are reported in Table II. The collapse of the data is superb. In Fig. 6(b) we plot $A_2M^{1/2}M_0^{3/2}N_A^{-1}b^{-3}$ versus z on a log–log plot. The constant C_2 is determined to be

$$C_2=2.02\pm0.08 \tag{20}$$

such that the crossover from θ to good solvent behavior occurs at $z_{\mathrm{th}}=1$ or when there is one thermal blob per chain. It is interesting to compare the value for the crossover of the thermal blob interaction parameter $z_{\mathrm{th}}=1$ with that for the conventional interaction parameter z

$$z=\left(\frac{2}{3\pi}\right)^{3/2}\frac{v}{b^3}N^{1/2}=0.128z_{\mathrm{th}}. \tag{21}$$

This parameter remains smaller than unity until there will be at least 64 thermal blobs per chain.

Although the collapse of the data is excellent, it should be noted that the use of only short chains in the current study means that the simulation points do not extend very far into the good solvent region ($z_{\mathrm{th}}\lesssim 3$ for the simulation data while $z_{\mathrm{th}}\lesssim 60$ for the experimental data), and as a result further simulations to test the models ability to reproduce experimental data further outside the θ region, either by increasing temperature or chain length, are certainly warranted. There are also three solid lines displayed in Fig. 6(b). The first two show least squares fits to the data for $z_{\mathrm{th}}<1$ and $z_{\mathrm{th}}>1$, which yields a value of C_1

$$C_1=0.20\pm0.02 \tag{22}$$

and the continuous line shows the simple crossover function

$$A_2M^{1/2}\frac{M_0^{3/2}}{N_Ab^3}=(0.20\pm0.02)\left[\left(\frac{1}{z_{\mathrm{th}}}\right)^{\alpha}+\left(\frac{1}{z_{\mathrm{th}}^{0.528}}\right)^{\alpha}\right]^{-1/\alpha} \tag{23}$$

with $\alpha=2.64\pm0.04$. The excellent collapse of the experimental data obtained from three different experiments performed upon two polymers in three solvents and from three different model systems without the use of any adjustable parameters clearly confirms that Eq. (17), and the numerical values of C_1 and C_2 determined here, are truly universal, i.e., independent of the chemical details of the polymer and the solvent used, and of the numerical model used. This leads to the unique relation between the excluded volume parameter v of the Kuhn segment and reduced temperature

$$v=(0.78\pm0.06)b^3\left(\frac{T-\theta_n}{T}\right). \tag{24}$$

V. CONCLUSIONS AND DISCUSSION

In this paper we have presented a new simulation method, inspired by the analytical work of Grosberg and Kuznetsov,[20] to evaluate the second virial coefficient between polymers. This new method is applied to chains represented by Lennard-Jones beads with either rigid or flexible bonds. Unlike previous methods used to obtain the second virial coefficient,[6,7] the new method determines the effective intermolecular interaction by direct simulation of two polymers whose centers of mass are connected by a harmonic spring. The use of such a spring then allows the probability histogram of finding the two centers of mass as a function of separation to be accumulated relatively easily. By removing the contribution to the probability histogram due to the spring linking the centers of mass it is possible to obtain the effective intermolecular interaction and the second virial coefficient, A_2.

Initially, we have considered the simple case of a pair of Lennard-Jones particles, and show that the new method recovers the Lennard-Jones potential from the probability histograms accumulated by the computer simulations. Values of the second virial coefficient obtained by computer simulation

TABLE II. Mass, M_0 (in units of g mol^{-1} from experiment and m_0 from simulation), and length, b (in units of Å from experiment and σ from simulation), of Kuhn segments and θ temperature, θ_n (in units of °C from experiment and reduced units from simulation) for different molecular weights, M_w (in units of g mol^{-1} from experiment and m_0 from simulation), of polystyrene, PMMA, and our model polymers used to collapse the data shown in Fig. 6.

Polymer	Solvent	M_w	M_0	b	θ_n
Polystyrene	Decalin	4 400 000	728	18.0	15.2
		1 560 000	728	18.0	15.4
		1 050 000	728	18.0	15.2
		622 000	728	18.0	12.2
		186 000	728	18.0	15.0
		125 000	728	18.0	12.0
		48 200	728	18.0	14.2
Polystyrene	Cyclohexane	422 000	728	18.0	35.0
		171 000	728	18.0	35.0
		82 000	728	18.0	35.0
		43 900	728	18.0	35.0
		24 000	728	18.0	35.0
PMMA	Water+TBA	2 380 000	500	12.9	41.5
Rigid bonds	none	16	1.61	1.61	3.43
		8	1.59	1.59	3.40
Flexible bonds $k_{\mathrm{FENE}}=30\epsilon/\sigma^2$	none	16	1.52	1.63	3.14
		8	1.49	1.59	3.13
Flexible bonds $k_{\mathrm{FENE}}=10\epsilon/\sigma^2$	none	16	1.48	1.64	2.85
		8	1.45	1.61	2.85

and from the *exact* numerical evaluation are in excellent agreement, confirming that this method provides an accurate route to obtain second virial coefficients.

Applying the method to short homopolymer chains of length $n=1$, 3, 7, and 15 results in effective intermolecular interactions which display the same strong temperature and chain length dependence reported previously in good solvent conditions.[7] In poor solvent conditions the depth of the attractive minimum increases with increasing chain length while its location is shifted to larger separations. For sufficiently long chains and low temperatures an approximately constant negative effective intermolecular interaction is observed for short separations, indicating that the two chains attract each other so strongly that they coalesce in a single globule. The observation of this type of behavior illustrates a clear advantage for using the method proposed here, since direct simulation allows conformations where two chains coalesce to be sampled much more efficiently than by methods which grow two chain conformations independently.[6] Another advantage of the current method is that direct simulation of the two chains will allow evaluation of the effective intermolecular interaction to be undertaken in the presence of solvent. That said, system sizes will place restrictions upon the length of the chains and the solvent densities which may be investigated. These restrictions arise since long simulations are required to sample the probability histograms, and it therefore becomes desirable to use as small a simulation box as possible, thus reducing the number of solvent particles necessary to achieve the desired density. On the other hand, a lower limit of the simulation box size is imposed by the length of chain considered, since removal of the contribution to the probability histogram due to the spring linking the centers of mass requires that the histograms must be accumulated for distances beyond the range of the intermolecular interaction. For example, for a chain of length $n=15$ distances larger than 7σ must be sampled, and a simulation box whose side is longer than 14σ should thus be used. If a number density of 0.5 is required then this implies that in excess of 1500 solvent particles must be included in the simulation. Obviously such simulations will be very CPU intensive and we are currently investigating the feasibility of conducting these types of simulation using modern computational facilities and simulation methods.

Having obtained the effective intermolecular interaction, the second virial coefficient, A_2, is calculated. The models display behavior expected from analytical theories and previous simulation studies. At high temperatures A_2 is positive, clearly demonstrating that repulsive interactions are dominant, and is a monotonically decreasing function of chain length. As the temperature is reduced A_2 becomes negative, demonstrating that attractive interactions become dominant with lowering temperature. The θ temperature, defined as the temperature at which the second virial vanishes, for each model shows linear behavior when plotted versus $n^{-1/2}$. Least squares fits to the θ temperature, of the form $k_B\theta_n/\epsilon = Bn^{-1/2}+k_B\theta_\infty/\epsilon$, allowed the θ temperature of an infinitely long chain to be estimated as $k_B\theta_\infty/\epsilon=3.52\pm0.01$, 3.183 ± 0.008 and 2.856 ± 0.006 for models with rigid and flexible bonds (represented by the sum of the Lennard-Jones and FENE potentials) with $k_{\mathrm{FENE}}\sigma^2/\epsilon=30$ and 10, respectively, and $R_0=2\sigma$. Increasing the degree of the flexibility in the model also alters the n dependence of the θ temperature

with the absolute value of B decreasing, such that $B=-0.31\pm0.03$ for the model with rigid bonds, -0.14 ± 0.01 and 0.01 ± 0.01 for the models with flexible bonds and $k_{\mathrm{FENE}}\sigma^2/\epsilon=30$ and 10, respectively.

The reason for the observed n independence of the θ temperature for the model with flexible bonds and $k_{\mathrm{FENE}}=10\epsilon/\sigma^2$ is not clear since the second virial coefficient between two chains is obtained from a renormalization of two-, three-, etc., body interaction.[4] Such calculations predict that the n dependence of θ_n should be suppressed by decreasing the strength of three-body repulsions. However, the introduction of flexible bonds into our model results in the aspect ratio of the Kuhn segments remaining essentially unchanged ($b=1.61\sigma$ for the model with rigid bonds compared with $b=1.64\sigma$ for the model with flexible bonds and $k_{\mathrm{FENE}}=10\epsilon/\sigma^2$), and it is therefore expected that the strength of three-body repulsions will be similar in these models. That said, determination of the θ temperature from conformational properties of the bond-fluctuation model[19] also indicates that the introduction of flexible bonds suppresses the n dependence of θ_n.

The suppression of the n dependence of θ_n for the model polymer chain with flexible bonds and $k_{\mathrm{FENE}}=10\epsilon/\sigma^2$ makes this model an ideal candidate for further study since in experimental systems the θ temperature either displays no n dependence or very weak n dependence. Furthermore, this model is ideal for a detailed examination of the conformational properties since the location of θ temperature is now known for all chain lengths. Thus comparison of the value $k_B\theta_n/\epsilon=k_B\theta_\infty/\epsilon=2.856\pm0.006$ obtained here with methods typically used to determine the θ temperature from conformational properties, along with comparison with theoretical predictions, may be made with relative ease. Such a study has been undertaken and the results will be presented in Paper II.[18]

Finally, we have compared our numerical results of the second virial coefficient with experimental results and show that the simulation data may be collapsed onto the experimental data without the use of any adjustable parameters. This process leads to the following universal functions of the second virial coefficient, A_2,

$$A_2M^{1/2}\frac{M_0^{3/2}}{N_Ab^3}=\begin{cases}(0.39\pm0.03)\left(N^{1/2}\dfrac{T-\theta_n}{T}\right) & (\theta\ \text{solvent})\\ (0.28\pm0.01)\left(N^{1/2}\dfrac{T-\theta_n}{T}\right)^{0.528} & (\text{good solvent})\end{cases} \tag{25}$$

$$=(0.20\pm0.02)\begin{cases}z_{\mathrm{th}} & (z_{\mathrm{th}}<1,\ \theta\ \text{solvent})\\ z_{\mathrm{th}}^{0.528} & (z_{\mathrm{th}}>1,\ \text{good solvent})\end{cases} \tag{26}$$

$$=(0.20\pm0.02)\left[\left(\frac{1}{z_{\mathrm{th}}}\right)^{2.6}+\left(\frac{1}{z_{\mathrm{th}}^{0.528}}\right)^{2.6}\right]^{-1/2.6}, \tag{27}$$

where M_0 and b are the mass and length of a Kuhn segment, respectively. Furthermore, Eqs. (25) and (9) leads to an excluded volume of a Kuhn segment,

$$v=(0.78\pm0.06)b^3\left(\frac{T-\theta_n}{T}\right). \tag{28}$$

In Paper II[18] we will show that this relation, used within the mean-field Flory theory, successfully predicts the size of the model polymer chains at temperatures close to the θ temperature.

The observation of superb collapse of the data clearly shows that these are truly universal functions and may therefore be applied to any linear homopolymer independent of it chemical details and type of solvent without alteration of the prefactors in Eqs. (25)–(27).

ACKNOWLEDGMENTS

The material is based upon work supported by the STC Program of the National Science Foundation under Agreement No. CHE-9876674, and by the NSF under Grant No. DMR-0102267. We also wish to acknowledge the North Carolina Super Computer Center for an award of CPU time on the IBM SP. This work has benefitted from discussions with Dr. M. Adam and Dr. R. Colby, and we thank them for their contributions.

[1] P. J. Flory, *Principles of Polymer Chemistry* (Cornell University Press, Ithaca, NY, 1967).
[2] P. J. Flory, *Statistical Mechanics of Chain Molecules* (Interscience, New York, 1969).
[3] H. Yamakawa, *Modern Theory of Polymer Solution* (Harper and Row, New York, 1971).
[4] J. des Cloizeaux and G. Jannink, *Polymers in Solution: Their Modeling and Structure* (Claredon, Oxford, 1990).
[5] Refs. 1–28 of Paper II (Ref. 18).
[6] J. Dautenhahn and C. K. Hall, Macromolecules **27**, 5399 (1994).
[7] V. I. Harismiadis and I. Szleifer, Mol. Phys. **81**, 851 (1994).
[8] P. Grassberger and R. Hegger, J. Chem. Phys. **102**, 6881 (1995).
[9] A. M. Rubio and J. J. Freire, Macromolecules **29**, 6946 (1996).
[10] A. M. Rubio and J. J. Freire, J. Chem. Phys. **106**, 5638 (1997).
[11] L. Leu and J. M. Prausnitz, Macromolecules **30**, 6650 (1997).
[12] Y. C. Chiew and V. Sabesan, Fluid Phase Equilib. **155**, 75 (1999).
[13] C. Vega, J. M. Labaig, L. G. MacDowell, and E. Sanz, J. Chem. Phys. **113**, 10398 (2000).
[14] P. G. Bolhuis, A. A. Loius, J. P. Hansen, and E. J. Meijer, J. Chem. Phys. **114**, 4296 (2001).
[15] G. Swislow, S.-T. Sun, I. Nishio, and T. Tanaka, Phys. Rev. Lett. **44**, 796 (1980).
[16] G. C. Berry, J. Chem. Phys. **44**, 4550 (1966).
[17] Y. Nakamura, T. Norisuya, and A. Teramoto, Macromolecules **24**, 4904 (1991).
[18] I. M. Withers, A. V. Dobryniń, and M. Rubinstein, J. Chem. Phys. (to be published).
[19] M. Wittkop, S. Kreitmeier, and D. Göritz, J. Chem. Phys. **104**, 3373 (1996).
[20] A. Y. Grosberg and D. V. Kuznetsov, J. Phys. II **2**, 1327 (1992).
[21] D. A. McQuarrie, *Statistical Thermodynamics* (Harper & Row, New York, 1976).
[22] D. Frenkel and B. Smit, *Understanding Molecular Simulation—From Algorithms to Applications* (Academic, London, 1996).
[23] E. Marinari and G. Parisi, Europhys. Lett. **19**, 451 (1992).

[24] W. T. Vetterling W. H. Press, S. A. Teukolsky, and B. P. Flannery, *Numerical Recipies*, 2nd ed. (Cambridge University Press, Cambridge, 1992).
[25] P. J. Flory and W. R. Krigbaum, J. Chem. Phys. **18**, 1086 (1950).
[26] A. Y. Grosberg, P. G. Khalatur, and A. R. Khokhlov, Makromol. Chem., Rapid Commun. **3**, 709 (1982).
[27] A. Baumgärtner, J. Chem. Phys. **72**, 871 (1980).
[28] I. Szleifer, E. M. O'Toole, and A. Z. Panagiotopoulos, J. Chem. Phys. **97**, 6802 (1992).
[29] R. Perzynski. Ph.D. thesis, Universite Paris VI, 1984.
[30] M. Nakata, Phys. Rev. E **51**, 5770 (1995).
[31] L. H. Sperling, *Introduction to Physical Polymer Science* (Wiley, New York, 1992).

The Journal of Chemical Physics is copyrighted by the American Institute of Physics (AIP). Redistribution of journal material is subject to the AIP online journal license and/or AIP copyright. For more information, see http://ojps.aip.org/jcpo/jcpcr/jsp
Copyright of Journal of Chemical Physics is the property of American Institute of Physics and its content may not be copied or emailed to multiple sites or posted to a listserv without the copyright holder's express written permission. However, users may print, download, or email articles for individual use.